Adsorption (2024) 30:827–840
https://doi.org/10.1007/s10450-024-00474-7

Mitigation of hazardous ammonia and hydrogen sulphide emissions using carbon based nanometal oxides adsorbents

Guadalupe Montserrat Valdes Labrada[1] · Ruth Azar[1] · Bernardo Predicala[2] · Mehdi Nemati[1]

Received: 27 December 2022 / Revised: 30 March 2024 / Accepted: 2 April 2024 / Published online: 14 April 2024

Abstract

Carbon based nano TiO_2-ZnO composite adsorbents were developed and evaluated for simultaneous adsorption of ammonia (NH_3) and hydrogen sulphide (H_2S). Screening of composites with different ZnO and TiO_2 loadings in terms of adsorption capacities identified a composite with 10% ZnO and 5% TiO_2 (10ZnO-5TiO_2-AC) as the most suitable. Breakthrough experiments with pre-mixed gases containing 50 to 550 mg L^{-1} of each NH_3 and H_2S at 22 to 280 °C showed that increase in NH_3 and H_2S concentrations led to higher equilibrium adsorption capacities for both gases. Increase of temperature decreased NH_3 equilibrium adsorption capacity but for H_2S higher values were observed at higher temperatures. The highest equilibrium adsorption capacity of 5.71 mg NH_3 g^{-1} was obtained with a mixture of 500 ppmv NH_3 and 550 ppmv H_2S at 22 °C, while for H_2S the highest value of 29.64 mg H_2S g^{-1} was seen with a mixture of 300 ppmv NH_3 and 300 ppmv H_2S at 280 °C. Multicomponent Langmuir isotherm described the simultaneous adsorption of NH_3 and H_2S with the high level of accuracy. The negative value of enthalpy of adsorption for NH_3 confirmed the exothermic and potentially physical nature of ammonia adsorption, while a positive value for H_2S adsorption pointed out to the endothermic and chemisorption nature of this process. Examination of fresh and exposed composite adsorbents by XRD and FTIR confirmed the chemical nature of H_2S adsorption.

Keywords NH_3 and H_2S emissions · Nano metal oxides · Carbon-based nanoadsorbent · Multicomponent isotherm

1 Introduction

Ammonia (NH_3) and hydrogen sulphide (H_2S) are two toxic and environmentally hazardous gases that co-exist in emissions from livestock operations, landfills, wastewater treatment plants and sewage sludge [5, 9, 13, 26]. Simultaneous presence of ammonia and hydrogen sulphide in biogas, fuel gases generated from biomass gasification and coke oven gas is also well documented [5, 13]. Concentrations of NH_3 and H_2S in these emissions depend on the source and could vary in the range 2–14,000 and 4-2174 ppm, respectively [9, 13]. Apart from detrimental effects on the human and animal health and severe corrosivity that could damage transportation and storage equipment, NH_3 and H_2S emissions contribute to the formation of primary air pollutants such as SO_x and NO_x, and other air pollutants classified as photochemical oxidants. Processes for the treatment of gases contaminated with both NH_3 and H_2S can be classified as biological and physicochemical processes. Application of biological processes have been reported for treating a mixture of NH_3, H_2S, butyric acid, and ethyl mercaptan [9], removal of NH_3 and H_2S from wastewater treatment plant emissions [2], tannery emissions [8], odorous gases from a domestic waste landfill site [29], raw biogas [5], and for the deodorization of compost [10]. The focal point of physicochemical treatments has been mainly on adsorption of NH_3 and H_2S by carbon-based adsorbents [3, 6] and catalytic oxidation by metal oxides [14, 15, 20]. A close look at previous studies on simultaneous removal of NH_3 and H_2S by carbon-based adsorbents and metal oxide catalyst-sorbent, as outlined in a recent review article [13] reveals that these works have been conducted at high gas concentrations (5000 ppmv NH_3 and 10,000 ppmv H_2S) and high temperatures (650 to 800 °C).

✉ Mehdi Nemati
Mehdi.Nemati@usask.ca

[1] Department of Chemical and Biological Engineering, University of Saskatchewan, 57 Campus Drive, Saskatoon, SK S7N 5A9, Canada

[2] Prairie Swine Centre Inc, 2105–8th St. E, P.O. Box 21057, Saskatoon, SK S7H 5N9, Canada

Considering that in many practical cases such as emissions from livestock operations, raw biogas, and emissions from landfills much lower concentrations of NH_3 and H_2S are encountered and the emitted gases are at lower temperatures, it is important to investigate the simultaneous removal of NH_3 and H_2S for the lower ranges of concentration and temperature and verify the effects of gas concentration and temperature on the effectiveness of the treatment process.

As part of an earlier work, we have investigated the effectiveness of pure (commercial) TiO_2 and ZnO nanoparticles mixture for simultaneous removal of NH_3 and H_2S from gases simulating the emissions from livestock operations for a range of gas mixture concentrations and temperatures [26]. Given the challenges associated with the use and handling of pure nanoparticles in large-scale treatment systems and their high cost, in the present work carbon-based nano metal oxide adsorbents, hereinafter referred to as ZnO-TiO_2-AC, were synthesized and used for simultaneous capture of NH_3 and H_2S. Effects of NH_3 and H_2S concentrations (50–500 mg L^{-1} of each gas in mixture) and temperature (22–280 °C) on the adsorption process were investigated. Examination of fresh and exposed adsorbents with XRD and FTIR allowed us to develop an insight on the nature of adsorption processes. Finally, the Langmuir multicomponent adsorption isotherm was used to describe the simultaneous adsorption of NH_3 and H_2S and the important adsorption and thermodynamic parameters were determined.

2 Materials and methods

2.1 Chemicals and gases

Zinc nitrate hexahydrate (98%, $Zn(NO_3)_2{\cdot}6H_2O$; CAS# 10196-18-6) and titanium isopropoxide (97%, $Ti[OCH(CH_3)_2]_4$; CAS# 546-68-9) were obtained from Sigma-Aldrich and used as precursors of zinc oxide (ZnO) and titanium oxide (TiO_2), respectively. Activated charcoal (Darco G-60; CAS# 7440-44-0) with 100 mesh size (particle size < 0.149 mm) was from Fisher Scientific and used together with zinc nitrate hexahydrate and titanium isopropoxide to synthetize the ZnO-TiO_2-AC composite adsorbents. Ammonia (1000 ppmv) and hydrogen sulfide (1000 ppmv) gases, each balanced with He, and industrial grade He (99.99%) were obtained from Air Liquide, and PraxAir, Canada, respectively and used to perform the adsorption experiments.

2.2 Synthesis of nano ZnO-TiO_2-AC composite adsorbents

Sol-gel method was used for the synthesis of nano ZnO-TiO_2-AC adsorbents with different compositions of 10% ZnO and 5% TiO_2, 15% ZnO and 5% TiO_2 and 15% ZnO and 10% TiO_2.The synthesis was carried out using two solutions containing the TiO_2 and ZnO precursors at the stoichiometric level required for the designated metal oxide loading on 10 g activated carbon [16]. Solution A was prepared by dissolving the stoichiometric quantity of titanium isopropoxide (as TiO_2 precursor) in 30 mL pure ethanol. Solution B was made by dissolving the stoichiometric amount of zinc nitrate hexahydrate (as ZnO precursor) in a mixture of 67.5 mL pure ethanol, 2 mL of acetic acid, and 7.2 mL of deionized water. The dissolution in either case was done by vigorous mixing at room temperature for one hour. This was followed by drop-wise addition of solution A to solution B and mixing over a period 30 min until a homogeneous solution was obtained. Activated carbon (10 g) was then added to this solution. The mixture was stirred for 2 h and left at room temperature for 24 h for gelation to occur. The resulting gel was separated from the liquid by vacuum filtration and washed with ethanol and water. The gel was dried at 120 °C for 12 h and calcined at 450 °C for 2 h under Argon atmosphere. Finally, the calcined solid (ZnO-TiO_2-AC composite) was crushed and sieved to obtain a powder with 100 mesh particle size [22]. The prepared composites were analyzed for ZnO and TiO_2 contents by an external laboratory (SRC Geoanalytical Laboratories, SK, Canada).

2.3 Experimental set-up for adsorption study

The adsorption experimental set-up used in this work has been described elsewhere [26]. In summary, as shown in Fig. 1, the main part of the experimental set-up was a pyrex glass adsorption column (diameter: 1.27 cm and height: 29.5 cm) that was equipped with heating tape (HTS-Amptek Co., USA) and a temperature controller (Omega K type, Stamford, USA), a differential pressure transducer and pressure gauges (Honeywell, USA). Three gas cylinders containing NH_3 (1000 ppmv, balanced with He), H_2S (1000 ppmv, balanced with He), and He (99.99% purity) with stainless steel connection tubes and associated mass flow controllers (Model GFC17, Aalborg Instruments and Controls, USA) were used to supply the feed gas mixtures with the designated composition into the adsorption column [26]. The treated gas (outlet) was connected to a gas chromatograph for real time measurement of NH_3 and H_2S concentrations. A bypass line and two valves were devised to determine the concentrations of NH_3 and H_2S in the feed (inlet) gas. To

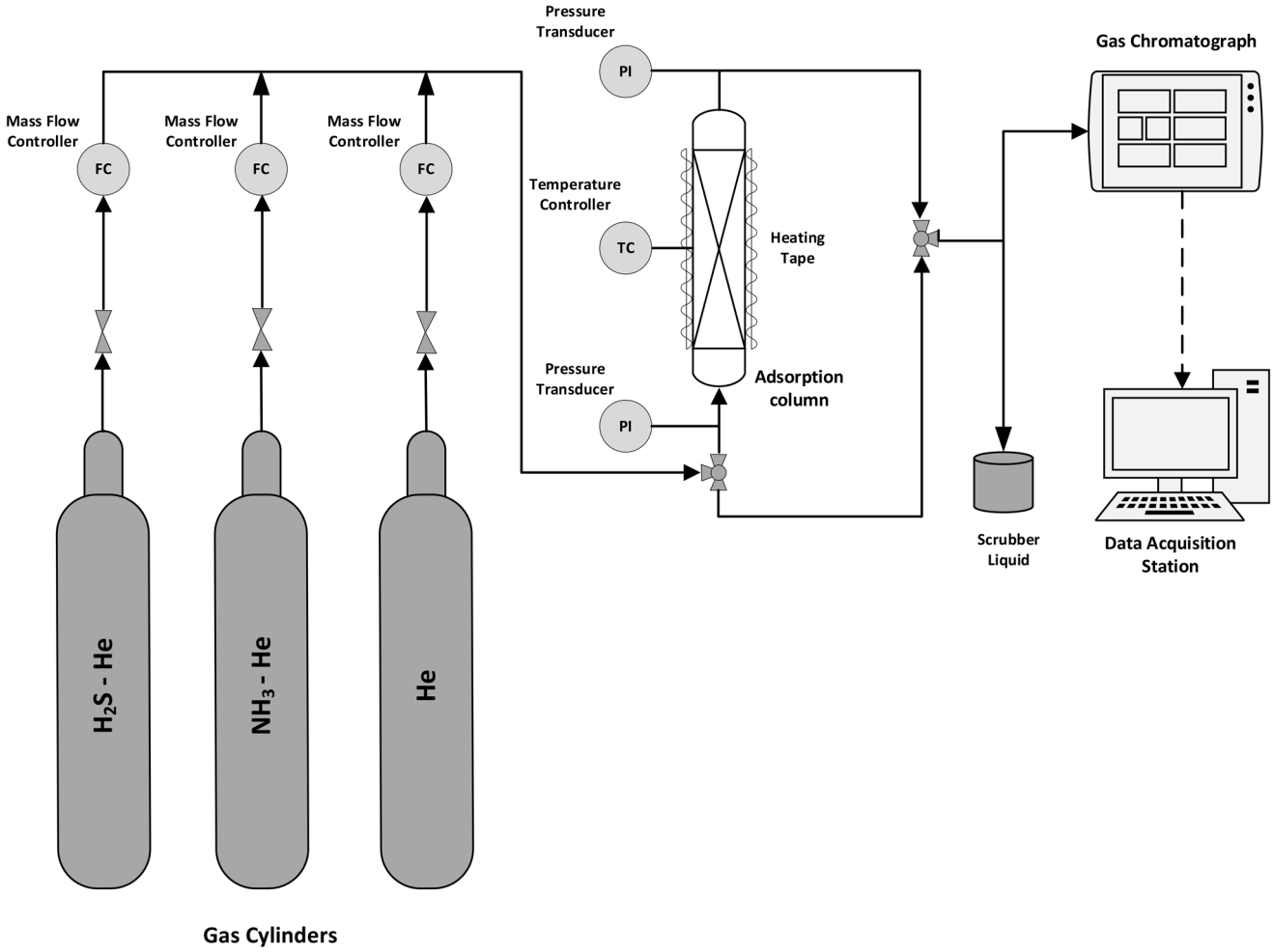

Fig. 1 Schematic flow diagram of the experimental set-up

prevent unintentional release of the hazardous gases into the environment and ensure safety, the experimental set-up and gas cylinders were placed inside a walk-in fume hood.

2.4 Experimental procedures

Adsorption experiments were carried out in two parts. First, the synthesized ZnO-TiO_2-AC composites of different composition were evaluated for their ability in simultaneous removal of NH_3 and H_2S. This was done by conducting adsorption experiments at room temperature (22 °C), using a feed gas mixture with 500 ppmv NH_3 and 550 ppmv H_2S, balanced with He. A set of control experiments was also conducted with activated carbon (no ZnO or TiO_2) that had undergone calcination, crushing and sieving in a similar fashion to that of composite adsorbents. The composite with the best performance in terms of NH_3 and H_2S adsorption capacities and preferably lower ZnO and TiO_2 contents was then identified and used for evaluating the effects of NH_3 and H_2S concentrations (50–50, 100–100, 200–200, 300–300, 400–400, 500–550 ppmv NH_3 and H_2S) and temperature (22, 70, 140 and 280 °C) on simultaneous removal of NH_3 and H_2S. The evaluated NH_3 and H_2S concentrations (50–500 ppmv) and temperatures (22–280 °C) covered the typical values observed in the emissions from livestock operations and industrial settings such as wastewater treatment plants and anaerobic digesters for production of biogas. Additionally, they were consistent with those applied in our previous work on simultaneous removal of NH_3 and H_2S with commercial (pure) ZnO and TiO_2 nanoparticles [26], thus allowing the comparison of the results. It should be emphasized that at each temperature all five gas combinations were tested.

The experimental procedure was the same in all cases and included the loading of adsorption column with a mixture of 0.2 g composite adsorbent and 0.8 g silicon carbide (125 micron). The rational for addition of silicon carbide and the chosen ratio is given elsewhere [23, 26]. To support the adsorbent and to prevent its carry over by the flowing gas, the absorbent was sandwiched between two layers

of glass wool followed by glass beads that filled the empty space below and above the adsorbent layer [23, 26]. The adsorption column was heated at 70 °C under helium flow for one hour to remove any adsorbed water. This was followed by adjusting the temperature to desired value and introducing the gas mixture with the designated composition into the column at a total flow rate of 100 ± 0.2 mL min^{-1} [23]. The concentrations of NH_3 and H_2S in the outlet gas was monitored in real time, using the gas chromatograph. Experimental run was stopped once breakthrough for both gases occurred (i.e., less than 1% change in NH_3 and H_2S concentrations). Concentrations of NH_3 and H_2S in the inlet gas (feed) were also measured at the beginning, during and at the end of each experimental run to ensure there was no deviation from the designated values. Another set of control experiments was conducted with calcined AC with a gas mixture containing 500 ppmv NH_3-550 ppmv H_2S at 22, 70, 140, and 280 °C.

The experimental data generated in each run were used to calculate the equilibrium adsorption capacities for NH_3 and H_2S. This was done by numerical integration of breakthrough curves, using MATLAB R2006a software. Calculation procedure including the relevant mathematical expression have been described elsewhere [23]. The fresh (unused) and spent adsorbents after exposure to 500 ppmv NH_3 and 550 ppmv H_2S at 22 and 280 °C (lowest and highest temperatures) were examined for their BET surface area and pore volume, X-ray diffraction (XRD), and FT-IR spectra. The fresh (unused) adsorbent was also examined by transmission electron microscopy (TEM) to determine the particle size distribution of metal oxides on activated carbon.

2.5 Analysis and characterization methods

A Varian Gas Chromatograph (Varian 3800, USA) with a thermal conductivity detector (TCD) connected to a CP-Pora PLOT Amines column (Agilent Technologies, CP7591) was used to measure the concentrations of NH_3 and H_2S in real time. The GC oven and TCD filament temperatures were set at 120 °C and 220 °C, respectively. The carrier gas flowrate (helium) was maintained at 10 mL min^{-1} and a split ratio of 1 was used. Automatic gas sampling was carried out in 6.5 min intervals which allowed sufficient time for elution of NH_3 and H_2S, before the next sampling event [26]. .

BET surface area and pore volume of fresh and selected exposed composite adsorbents were determined by a Micrometrics ASAP 2000 instrument. BET surface was determined using adsorption data for nitrogen at partial pressures of 0.05 and 0.3 (P/P_{atm}). Total pore volume was calculated using the amount of nitrogen adsorbed at a partial pressure of 0.95. Fresh and selected exposed composites were also examined by a D8-Advance Brucker Diffractometer XRD with a Cu Kα detector (Brucker, USA), and a Fourier-Transform Infrared (FTIR) spectrometer (Bruker Vertex 70, USA). The 2θ range for the XRD was 10–80° with a step size of 0.02°, and the FTIR was employed in the range of 400–4000 cm^{-1} at 4 cm^{-1} resolution. Finally, the unused composite adsorbent was examined by transmission electron microscopy (TEM), using a microscope (JEOL, 200 kV, USA), equipped with EDAX energy dispersive X-ray system (Genesis, USA) for EDS analysis. TEM micrographs were analyzed by Microstructure Measurement software to generate the particle size distribution of metal oxides.

3 Results and discussion

3.1 Performance of synthesized composite adsorbents

Figure 2 presents the NH_3 and H_2S breakthrough curves obtained with synthetized composites and calcinated activated carbon. Information on the metal oxides loading of each synthesized adsorbent and important adsorption characteristics including breakthrough times and equilibrium adsorption capacities for each adsorbent are provided in Table 1. Measurement of ZnO and TiO_2 contents of the synthesized adsorbents showed that the actual metal oxide loadings deviated slightly from the nominal loadings, despite the careful preparation and post treatment. Examination of the breakthrough curves and the associated data that are included in Table 1 showed that with all synthesized adsorbents, H_2S breakthrough time was shorter than that for NH_3. In case of calcined AC, the breakthrough of NH_3 and H_2S occurred closely but the breakthrough times were substantially shorter than those observed with the composites, indicating better performance of the composite adsorbents.

As far as the equilibrium adsorption capacities were concerned, all adsorbents including calcined AC displayed substantially higher capacities for H_2S when compared with NH_3. To be more specific, the H_2S adsorption capacities with all composite adsorbents were 4–5 folds higher than that for NH_3 and more than 7 folds higher with AC. Among the three synthesized composites, the 10ZnO-5TiO_2-AC composite showed the highest NH_3 and H_2S equilibrium adsorption capacities, despite the lowest metal oxides content. The adsorption capacities obtained for 15ZnO-5TiO_2-AC and 15ZnO-10TiO_2-AC were close. The observed NH_3 adsorption capacity of 10ZnO-5 TiO_2-AC composite was 61% higher than that of calcined activated carbon (5.30 vs. 3.29 mg NH_3 g^{-1}) but was around 5% lower in the case of H_2S (22.24 vs. 23.67 mg H_2S g^{-1}). It is also important to re-emphasize that the breakthrough times with this composite

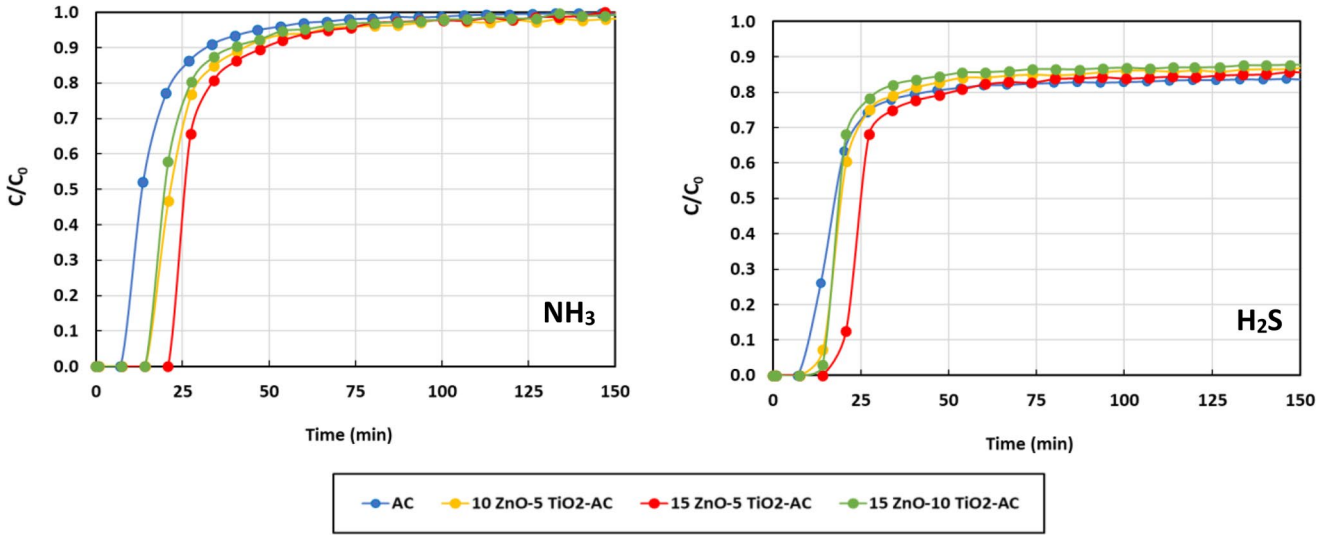

Fig. 2 Ammonia (left panel) and hydrogen sulphide (right panel) breakthrough curves for synthesized ZnO-TiO_2-AC composites and calcined activated carbon (AC). Inlet gas composition: 500 ppmv NH_3-550ppmv H_2S- balanced He, temperature: 22 °C

Table 1 Comparison of breakthrough times and adsorption capacities of ZnO-TiO_2-AC composites with different ZnO and TiO_2 loadings. Adsorption experiments were conducted with a feed gas mixture of 500 ppmv NH_3-550ppmv H_2S at 22 °C. Data for calcined AC included in this table have been obtained under similar conditions

Adsorbent	Nominal loading of ZnO and TiO_2 (%)	Actual loading of ZnO and TiO_2 (%)	NH_3 breakthrough time (min)	Equilibrium adsorption capacity(mg NH_3 g^{-1})	H_2S breakthrough time(min)	Equilibrium adsorption capacity(mg H_2S g^{-1})
10ZnO-5TiO_2-AC	10 and 5%	8.4 and 6.0%	14.1	5.30	11.5	22.24
15ZnO-5TiO_2-AC	15 and 5%	15.8 and 5.6%	20.8	4.50	14.1	21.57
15ZnO-10TiO_2-AC	15 and 10%	14.9 and 8.5%	14.1	4.22	13.5	21.33
Calcinated AC*	-	-	7.4	3.29	7.0	23.67

*AC: Activated carbon

were substantially higher that those for calcined AC (14.1 vs. 7.4 min for NH_3 and 11.5 vs. 7.0 min for H_2S). Given the better performance of 10ZnO-5TiO_2-AC and its lowest metal oxides contents, this composite adsorbent was selected to assess the effects of NH_3 and H_2S concentrations and temperature on simultaneous removal of these gases and for developing the adsorption isotherms.

3.2 Adsorption isotherms for 10ZnO-5TiO_2-AC composite

Figure 3 presents the NH_3 and H_2S breakthrough curves obtained with 10ZnO-5TiO_2-AC composite at different gas compositions and temperatures. The breakthrough times and equilibrium adsorption capacities for each set of conditions are summarized in Table 2. Ammonia breakthrough curves (Fig. 3, left panels) and data compiled in Table 2 show that increases in NH_3 concentration and temperature shifted the curves to the left, a clear indication of decrease in breakthrough time. The effect of NH_3 concentration on the breakthrough time was more pronounced at lower temperatures. For instance, at 22 °C the breakthrough time decreased from 120.7 to 13.8 min when NH_3 concentration increased from 50 to 500 ppmV but the corresponding values at 280 °C were 40.4 and 7.1 min, respectively. Based on the data compiled in Table 2, the equilibrium adsorption capacity of 10ZnO-5TiO_2-AC composite for NH_3 showed an increasing trend with increase of NH_3 concentration, but temperature had an opposing effect and lower adsorption capacities were seen with the increase in temperature. Specifically, the highest adsorption capacity of 4.60–5.71 mg NH_3 g^{-1} was achieved with 500 ppmv NH_3 at 22 °C.

As seen in Fig. 3 (right panels), the impact of H_2S concentration on breakthrough time was similar to that of NH_3 and shorter breakthrough times were observed as H_2S concentration was increased but there were several distinctions between NH_3 and H_2S. First, with 50 ppmv H_2S, breakthrough did not occur at 140 and 280 °C, even after a prolonged period of experiment. Second, the H_2S breakthrough curves were not as steep as those for NH_3 and although plateau region was observed, adsorbent never reached the saturation state ($C/C_0 = 1$) under any conditions. The ultimate

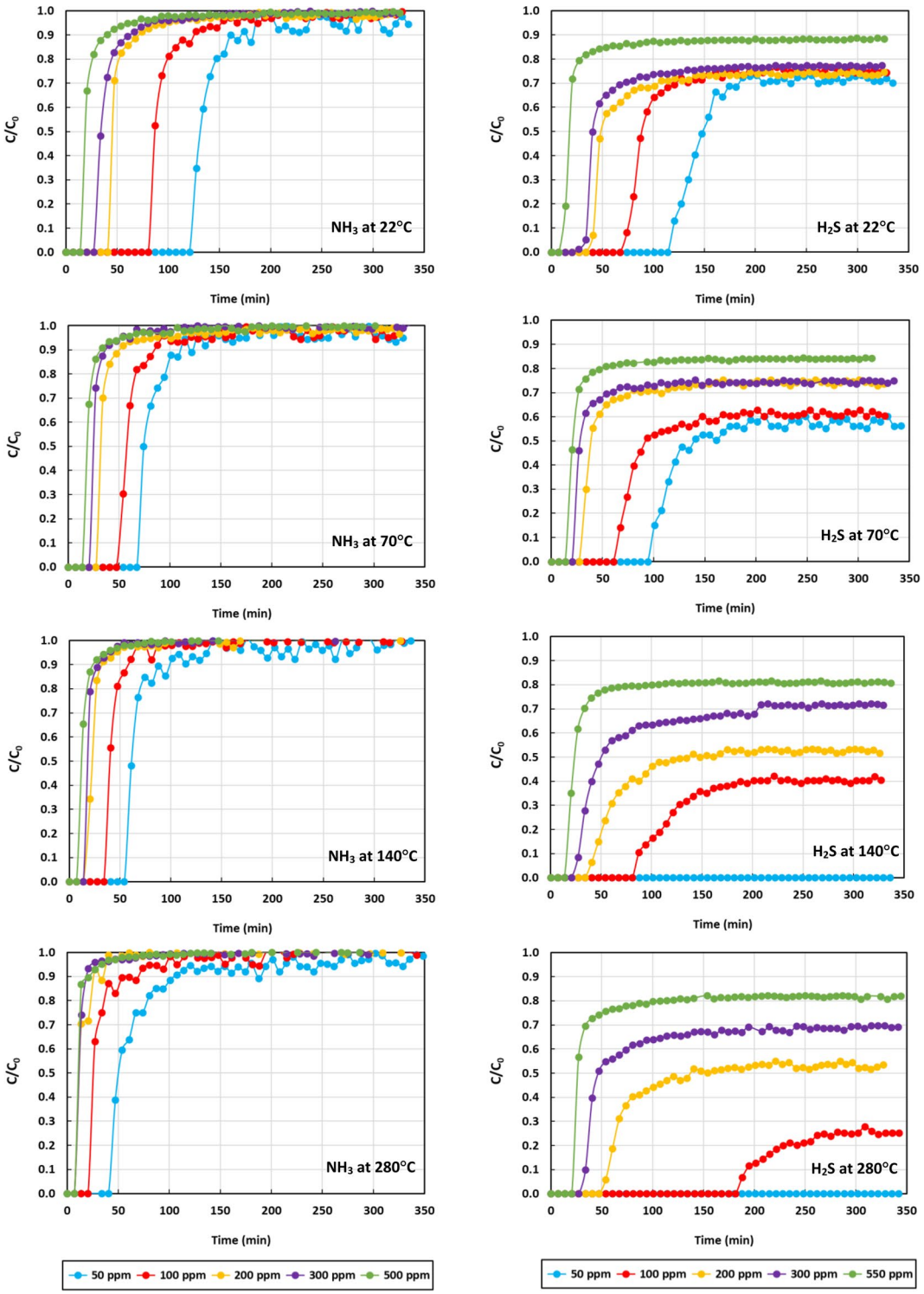

Fig. 3 Ammonia (left panels) and hydrogen sulphide (right panels) breakthrough curves obtained with 10ZnO-5TiO_2-AC composite adsorbent at different gas concentrations and temperatures

value of C/C_0 was dependent on concentration of H_2S, with the higher C/C_0 values observed at higher H_2S concentrations. These trends that are consistent with those obtained in our earlier work on with a mixture of pure ZnO and TiO_2 nanoparticles [26], is likely due to the chemical reaction between H_2S and ZnO (chemisorption) and the endothermic nature of this reaction, where higher temperatures lead to faster reaction rates. In fact, examination of the exposed

Table 2 Comparison of breakthrough times and adsorption capacities of composite 10ZnO-5TiO_2-AC, commercial (pure) ZnO and TiO_2 nanoparticles mixture [26], and calcined AC. Equilibrium adsorption capacities are not reported when breakthrough did not occur

		NH_3 breakthrough time(min)			Equilibrium adsorption capacity(mg NH_3 g^{-1})			H_2S breakthrough time(min)			Equilibrium adsorption capacity(mg H_2S g^{-1})		
NH_3-H_2S concentrations(ppmv)	**Temperature (°C)**	10 ZnO-5 TiO_2-AC	AC	ZnO & TiO_2mixture	10 ZnO-5 TiO_2-AC	AC	ZnO & TiO_2mixture[a]	10 ZnO-5 TiO_2-AC	AC	ZnO & TiO_2mixture[a]	10 ZnO-5 TiO_2-AC	AC	ZnO & TiO_2mixture[a]
50-50	22	120.7		358.9	2.54		6.92	114		199.7	6.74		14.55
	70	67.3		233	1.55		6.04	94.2		272.9	7.26		20.56
	140	54.0		246.8	1.31		5.22	-		446.3	-		-
	280	40.4		-	1.26		-	-		-	-		-
100-100	22	80.5		192.6	3.39		8.06	67.1		126.5	10.35		18.88
	70	47.2		153.4	2.28		6.9	60.6		153.4	12.1		28.49
	140	33.9		132.4	1.53		6.18	80.8		278.22	16.71		38.29
	280	20.3		40.7	1.24		1.35	181.4		604	21.45		-
200-200	22	40.7		100.9	3.72		9.67	34.0		40.8	17.15		19.23
	70	27.2		87.5	2.85		8.31	27.2		87.5	15.95		30.59
	140	13.7		60.4	1.56		7.41	33.8		139.9	18.34		49.36
	280	7.1		27.4	0.94		1.67	47.1		207.3	26.50		-
300-300	22	27.0		73.9	4.38		11.27	20.3		27.3	22.49		20.62
	70	20.4		67.3	2.95		10.14	20.4		34.1	22.25		30.21
	140	13.7		40.7	1.92		5.69	20.5		80.5	27.32		45.56
	280	7.1		27.5	1.41		3.7	27.3		193.6	29.64		-
500-550	22	13.8	7.0	27.5	4.60-5.71[b]	3.29	11.95	7.3	7.1	7.6	20.52-22.24[b]	23.67	27.21
	70	13.6	7.0	27.1	4.13	2.44	10.72	13.6	6.9	27.1	23.93	21.81	31.34
	140	7.0	6.9	27.5	2.43	1.87	8.4	13.6	7.1	67.3	26.70	22.6	52.31
	280	7.1	6.9	7.3	2.22	1.83	3.57	20.4	13.5	46.8	28.40	23.44	-

[a] The adsorption capacities reported by Valdes Labrada et al. [26] are calculated by assuming that NH_3 was exclusively adsorbed by TiO_2 nanoparticles and H_2S was adsorbed only by ZnO nanoparticles. [b] Experiments for this set were done twice

adsorbents by XRD and FTIR, as presented in the latter parts of this article, confirmed the validity of this speculation. The increase in H_2S concentration and temperature both enhanced the H_2S adsorption capacity of 10 ZnO-5 TiO_2-AC. This indicated that while the impact of concentration was similar to the the trend observed for NH_3, the temperature effect was opposite of that for NH_3.

Included in Table 2 are also the NH_3 and H_2S breakthrough times and equilibrium adsorption capacities obtained for the calcined activated carbon when exposed to a gas mixture containing 500 ppmv NH_3-550 ppmv H_2S at 22 to 280 °C (control experiments). Comparing these data with the corresponding values for 10ZnO-5TiO_2-AC composite reveals that the breakthrough times in the case of composite adsorbent in general are 1.5-2 times longer than those for calcined AC. Moreover, the loading of activated carbon with small quantities of ZnO (8.4%) and TiO_2 (6%) enhanced its capacity for simultaneous removal of NH_3 and H_2S, with the impact being more pronounced on adsorption capacity of NH_3. To be specific, the enhancement in NH_3 adsorption capacity was in the range 21–73%, with the most impact observed at 22 and 70 °C, while the enhancement in the case of H_2S was 10–21% with the effect being more pronounced at 140 and 280 °C. The only exception was the H_2S adsorption capacity at 22 °C that showed 6% decrease with the composite adsorbent.

Table 2 also provides the NH_3 and H_2S breakthrough times and equilibrium adsorption capacities obtained as part of an earlier work with the mixture of commercial (pure) ZnO and TiO_2 nanoparticles. As seen, the dependency of NH_3 and H_2S breakthrough times and adsorption capacities on gas concentration and temperature were consistent with the trends observed with 10ZnO-5TiO_2-AC composite. However, the breakthrough times with the mixture of commercial (pure) ZnO and TiO_2 nanoparticles were longer and the equilibrium adsorption capacities were also higher than those obtained with the composite. Given the small quantities of ZnO and TiO_2 in the composite adsorbent (8.4 and 6%, respectively), the higher adsorption capacities with mixture of pure ZnO and TiO_2 nanoparticles is not surprising.

To describe the equilibrium data obtained for simultaneous adsorption of NH_3 and H_2S on the composite adsorbent, multicomponent Langmuir isotherm, represented by Eqs. 1 and 2, was used:

$$q_i = \frac{q_{si} K_i P_i}{1 + K_i P_i + K_j P_j} \tag{1}$$

$$q_j = \frac{q_{sj} K_j P_j}{1 + K_i P_i + K_j P_j} \tag{2}$$

where q_i and q_j are the equilibrium adsorption capacities of NH_3 and H_2S (mg gas g^{-1}), P_i and P_j are the partial pressures of NH_3 and H_2S in the mixture (kPa), q_{si} and q_{sj} are the maximum adsorption capacities of NH_3 and H_2S, and K_i and K_j are the equilibrium constants for NH_3 and H_2S, respectively. The dependency of equilibrium constants on temperature was described by van't Hoff expression (Eqs. 3 and 4):

$$K_i = K_{0i} \exp\left(\frac{-\Delta H_i}{RT}\right) \tag{3}$$

$$K_j = K_{0j} \exp\left(\frac{-\Delta H_j}{RT}\right) \tag{4}$$

Substituting the K_i and K_j as defined by Eqs. 3 and 4 in the multicomponent Langmuir isotherm expressions (Eqs. 1and 2) results in the extended form of these expressions:

$$q_i = \frac{q_{si} K_{0i} \exp\left(\frac{-\Delta H_i}{RT}\right) P_i}{1 + K_{0i} \exp\left(\frac{-\Delta H_i}{RT}\right) P_i + K_{0j} \exp\left(\frac{-\Delta H_j}{RT}\right) + P_j} \tag{5}$$

$$q_j = \frac{q_{sj} K_{0j} \exp\left(\frac{-\Delta H_i}{RT}\right) P_j}{1 + K_{0i} \exp\left(\frac{-\Delta H_i}{RT}\right) P_i + K_{0j} \exp\left(\frac{-\Delta H_j}{RT}\right) + P_j} \tag{6}$$

where K_{0i} and K_{0j} are the pre-exponential factors (kPa^{-1}), ΔH_i and ΔH_j are the enthalpies of NH_3 and H_2S adsorptions (kJ mol^{-1}), respectively, T is temperature (K), and R is the universal gas constant (kJ mol^{-1} K^{-1}). The equilibrium data obtained for adsorption of NH_3 and H_2S at different temperatures were then fit non-isothermally into Eqs. 5 and 6 and the value of various coefficients were determined. This was done using the built-in Solver in Excel and by minimizing an objective function (Eq. 7), defined as the sum of squares of differences of experimentally determined adsorption capacities and those calculated by the isotherm expressions:

$$f = \sum_i \sum_j \left(q_{Exp.,ij} - q_{Calc.,ij}\right)^2 \tag{7}$$

The coefficient of determination (R^2) was determined from Eq. 8:

$$R^2 = 1 - \frac{\sum_i \sum_j \left(q_{Exp,ij} - q_{Calc,ij}\right)^2}{\sum_i \sum_j \left(q_{Exp,ij} - q_{mean}\right)^2} \tag{8}$$

The values of q_s, K_0, and ΔH for NH_3 and H_2S were 68.93 mg NH_3 g^{-1} and 34.31 mg H_2S g^{-1}, 2.26 and 518 kPa^{-1}, and

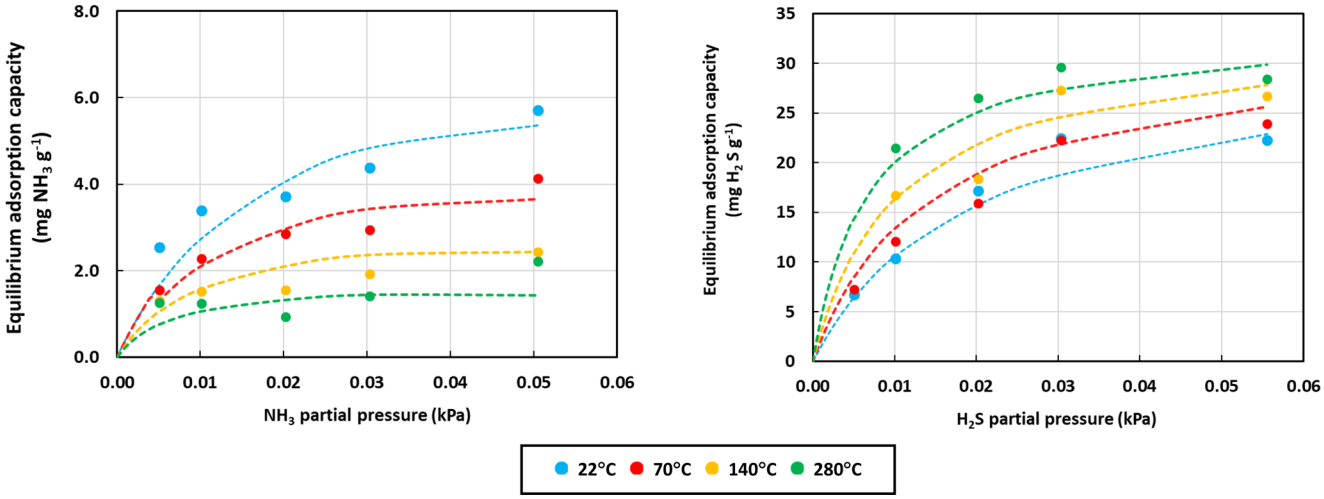

Fig. 4 Ammonia (left panels) and hydrogen sulphide (right panels) adsorption isotherms for 10ZnO-5TiO_2-AC composite adsorbent. Symbol are experimentally determined adsorption capacities and dashed lines are Langmuir multicomponent model predictions (goodness of fit)

Table 3 BET surface area, pore volume and average pore size of fresh 10ZnO-5TiO_2-AC composite adsorbent and the saturated composite adsorbents after exposure to 500 ppmv NH_3-550 ppmv H_2S at 22 °C and 280 °C

Adsorbent	BET surface area ($m^2\ g^{-1}$)	Pore volume ($cm^3\ g^{-1}$)	Pore size (nm)
Fresh	914.55	0.73	3.17
Exposed (22 °C)	903.15	0.73	3.27
Exposed (280 °C)	854.74	0.67	3.15

-2.40 and 5.83 kJ mol^{-1}, respectively. The experimentally determined NH_3 and H_2S equilibrium adsorption capacities and the corresponding predictions by the multicomponent Langmuir isotherm are contrasted in Fig. 4. The goodness of fit shown in this figure for both NH_3 and H_2S and an $R^2 = 98.1\%$ indicated that the multicomponent Langmuir model predicted the experimental data with high level of accuracy. The negative value of enthalpy of the adsorption for NH_3 (-2.4 kJ mol^{-1}), confirmed the exothermic and potentially physical nature of ammonia adsorption on 10ZnO-5TiO_2-AC, as reported in other works [22, 23], while in the case of H_2S a positive value for adsorption enthalpy showed the endothermic and chemisorption nature of H_2S adsorption.

3.3 Characterization of fresh and exposed 10ZnO-5TiO_2-AC adsorbents

Table 3 presents the BET surface area, pore volume and average pore size of the fresh 10ZnO-5TiO_2-AC composite and saturated adsorbents after exposure to 500 ppmv NH_3-550 ppmv H_2S at 22 °C and 280 °C. The fresh adsorbent had the highest BET surface area and pore volume (914.55 $m^2\ g^{-1}$ and 0.73 $cm^3\ g^{-1}$) which were both lower than the corresponding values for activated carbon (1122 $m^2\ g^{-1}$ and 0.91 $cm^3\ g^{-1}$), as reported earlier [22, 23]. This is expected and caused by the dispersion of ZnO and TiO_2 on the surface and pores of activated carbon [22, 23]. The exposure of the composite to NH_3 and H_2S decreased its surface area and pore volume, and the effect was pronounced at the higher temperature of 280 °C. As discussed in more details in the latter part of this section, the chemical nature of H_2S adsorption led to formation of ZnS, with the reaction being temperature dependent. Thus, the lower surface area and pore volumes observed for the exposed adsorbents, especially at 280 °C, is not caused only by the addition of ZnO and TiO_2, and the formation and deposition of ZnS on the activated carbon surface and pores is the other contributing factor.

TEM images of fresh 10ZnO-5TiO_2-AC composite adsorbent (Fig. 5, panels a, b) clearly show the presence and distribution of metal oxides on the activated carbon. The particles size distribution for metal oxide, obtained by analysis of TEM images, revealed that most of the metal oxide particles (70.6%) were in a size range of 0–2 nm and a smaller percentage (21.6%) were 3–9 nm particles. The largest particles detected on the composite were in the size range of 10–13 nm and accounted for 7.8% of all particles (Fig. 5, panel c).

Figure 6 presents the XRD spectra of fresh 10ZnO-5TiO_2-AC composite adsorbent and saturated composite adsorbents after exposure to 500 ppmv NH_3-550ppmv H_2S at 22 °C and 280 °C. In all three cases, peaks corresponding to activated carbon were observed at 20.8°, 21.95°, 26.6°, and 43.4° [22]. Presence of TiO_2 was also evident through peaks at 25.4°, 36.4°, 50.1°, 56.6° and 62.8° that were seen in fresh and exposed adsorbent spectra and matched those of anatase TiO_2 peaks as reported by

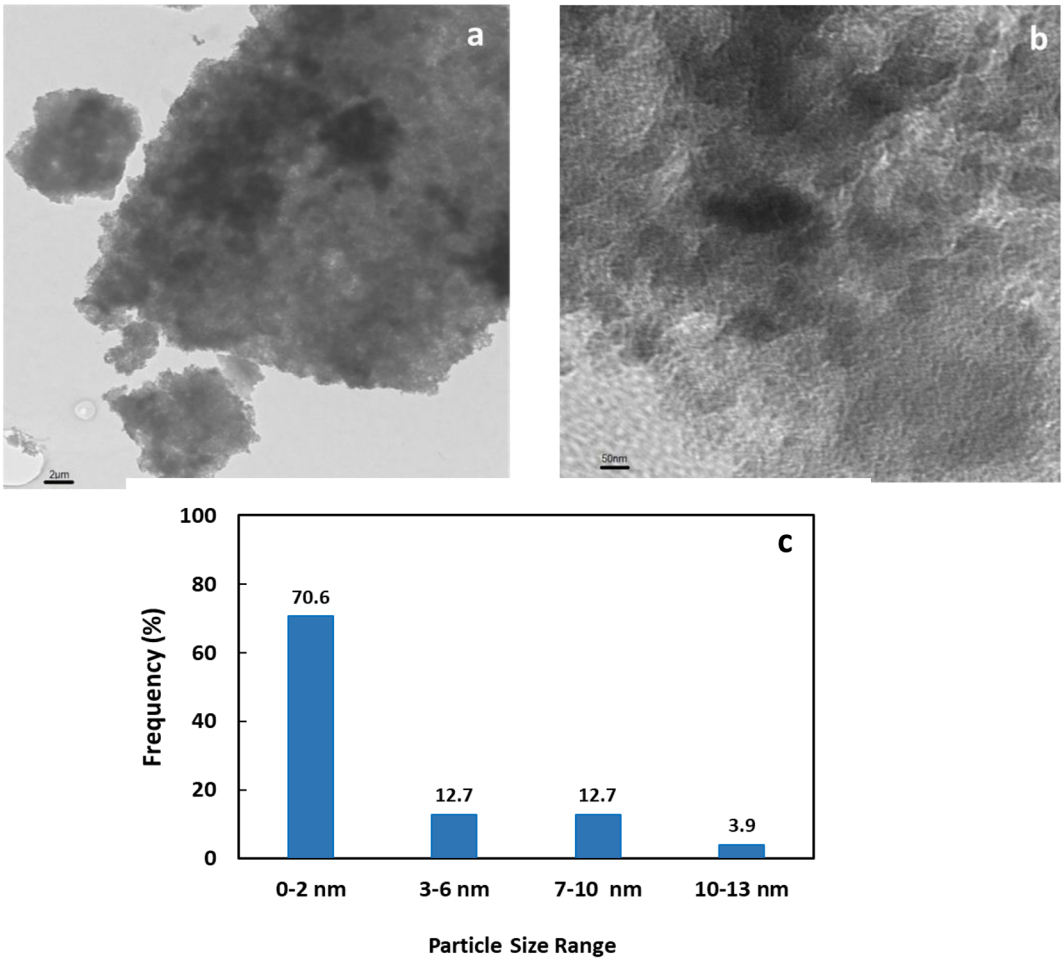

Fig. 5 TEM images of fresh 10ZnO-5TiO_2-AC composite adsorbent at two different magnifications (panels **a** and **b**) and particle size distribution of nanoparticles (panel **c**)

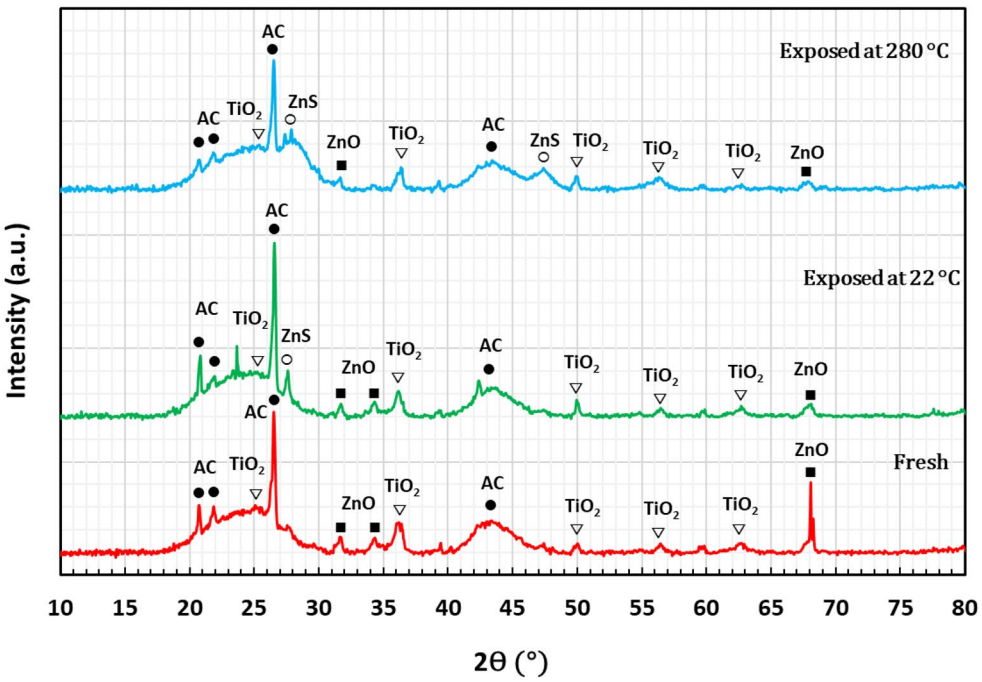

Fig. 6 XRD spectra of fresh 10ZnO-5TiO_2-AC composite adsorbent (red) and saturated adsorbents after exposure to 500 ppmv NH_3-550ppmv H_2S at 22 °C (green) and 280 °C (blue)

others [11, 19, 22, 27, 28]. Peaks at 31.7°, 34.4°, and 68.1° in the fresh adsorbent and those exposed to NH_3 and H_2S confirmed the presence of ZnO in the composite adsorbents [24]. Spectra of exposed adsorbents included a peak at 28.1° that corresponded to zinc sulfide (ZnS) and confirmed the chemisorption of H_2S on ZnO in accordance with Eq. 9 [21, 24–26].

$$ZnO\,(s) + H_2S\,(g) \rightarrow ZnS\,(s) + H_2O\,(g) \quad (9)$$

The chemisorption nature of H_2S adsorption was also supported by substantial decrease in intensity of ZnO peak at 68° in the exposed adsorbents, indicating the conversion of ZnO to ZnS. It is important to point out that in the case of adsorbent exposed to 500 ppmv NH_3-550ppmv H_2S at 280 °C, an additional peak that corresponds to ZnS polycrystalline structure is seen at 47.5° [12]. These evidence all point to endothermic chemisorption of H_2S adsorption, as confirmed by a positive value for enthalpy of H_2S adsorption described in Sect. 3.2.

The FTIR spectra of fresh 10ZnO-5TiO_2-AC composite adsorbent and saturated composite adsorbents after exposure to 500 ppmv NH_3-550ppmv H_2S mixture at 22 °C and 280 °C are shown in Fig. 7. The FTIR spectra in all three cases displayed the adsorption bands that are associated with oxygen-containing functional groups. The patterns in the region of 3900 and 3600 cm^{-1} is associated with O-H stretching of water [18] and/or -OH groups of alcohol or phenols on the activated carbon surface [7]. The broad band between 1600 and 1400 cm^{-1} is attributed to skeleton vibration of aromatic C=C groups and stretching of C=O in COOH groups on the surface of activated carbon [7, 18]. The strong band at 607 cm^{-1} observed in all three adsorbents corresponds to bulk titania skeletal [7]. The peak observed at 1060–1070 cm^{-1} is related to the Ti-O stretching and the surface conjugation between the activated carbon and the Ti-O bonds as Ti-O-C [4]. .

The peaks associated with the vibrational band of liquid ammonia, the hydrogen bonded ammonia to the surface Bronsted acid sites, and the symmetric bending mode (δ_{sym}) of ammonia molecules that are reported to occur at 1054 cm^{-1}, 1100 and 1105 cm^{-1}, and 1150 and 1236 cm^{-1}, respectively [23], all coincide with the broad band observed between 1600 and 1400 cm^{-1} in Fig. 7 that could indicate overlapping of carbon and ammonia related peaks in the exposed adsorbents. The peak at 2979 cm^{-1} that is only observed in the exposed sample coincides with the stretch of NH_3^+ species and the overtone of N-H vibration [17].

A peak that has been attributed to vibration Zn-O bonds (420–410 cm^{-1}) is clearly seen in the spectra of fresh adsorbent and adsorbent exposed to the mixture of NH_3 and H_2S at 22 °C but for the exposed adsorbent at 280 °C this peak is not visible. The reason for absence of this peak is the reaction of H_2S with ZnO and formation of ZnS according to Eq. 9, as demonstrated earlier by examining the XRD spectra of fresh and exposed adsorbents. The chemisorption of H_2S by ZnO is further supported by the existence of a peak at 559 cm^{-1} in the spectra of adsorbent exposed to NH_3 and H_2S at 280 °C that has been attributed to vibrations of ZnS bonds [1]. The small magnitude or absence of this peak in the case of adsorbent exposed to NH_3 and H_2S at 22 °C once again point to endothermic nature of this chemisorption process and the positive impact of higher temperatures on the reaction.

As indicated in the introduction, several recent works have been dedicated to simultaneous removal of NH_3 and

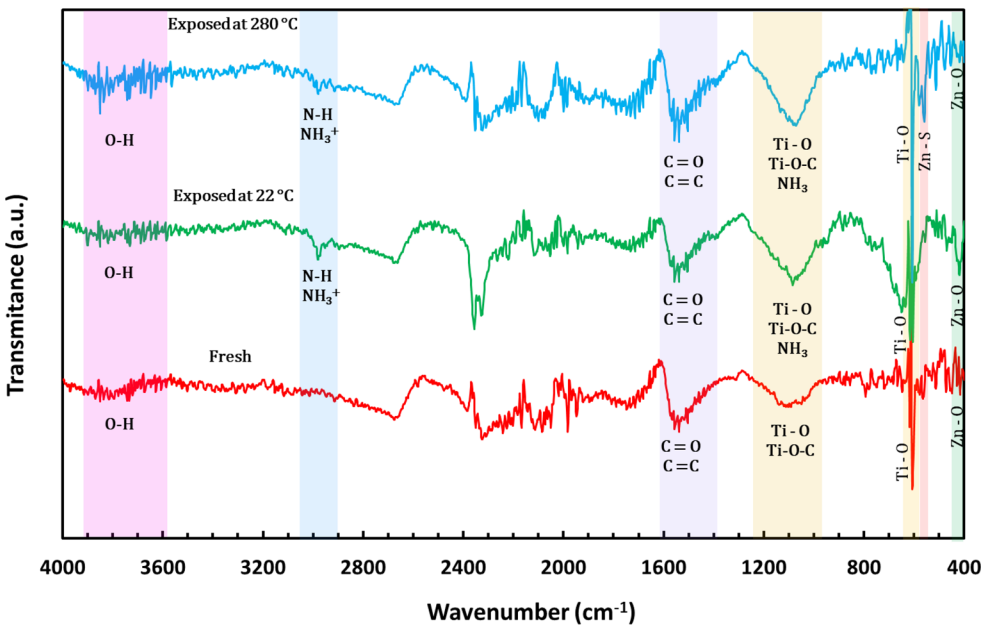

Fig. 7 FTIR spectra of fresh 10ZnO-5TiO_2-AC composite adsorbent (red) and saturated adsorbents after exposure to 500 ppmv NH_3-550ppmv H_2S at 22 °C (green) and 280 °C (blue)

H_2S from gaseous streams, using metal oxide catalyst-adsorbents. Jung et al. [14] used Zn–Al-based sorbents, promoted with cobalt, nickel and iron oxides for the removal of NH_3 and H_2S from coal-based synthesis gas that contained 5,000 ppmv NH_3 and 10,000 ppmv H_2S. The adsorption of H_2S (sulfidation) and decomposition of NH_3 before and after sulfidation process were evaluated in a micro-reactor at 1 atm and 650 °C with a gas flow rate of 50 mL h^{-1}. Cobalt, nickel and iron oxides were active components in decomposition of NH_3 and absorption of H_2S, while ZnO and Al_2O_3, major constituents of each adsorbent, did not show any activity in NH_3 decomposition. Among cobalt, nickel and iron oxides, cobalt oxide was most effective in decomposition of NH_3. In a follow-up study with hot coal gases under similar operating conditions, cobalt oxide, molybdenum oxide, and nickel oxide were all shown to be effective in decomposition of NH_3 alone but the presence of hydrogen sulfide and sulfidation reaction substantially decreased their effectiveness in removal of NH_3 [20]. To improve the removal of NH_3 and H_2S, Zn-based adsorbents with either cobalt, molybdenum, or nickel oxide were also evaluated. The Zn-based adsorbent CZ-30 that contained 30% cobalt oxide and 70% Zno outperformed the other two adsorbents, with the breakthrough capacities at 1 atm and 650 °C with 5000 ppmv NH_3 and 10,000 ppmv H_2S were reported as 88 mg NH_3 $g^{-1}$and 370–425 mg H_2S g^{-1}. Lim et al. [15] extended this work by impregnating Al_2O_3, SiO_2, and ZrO_2 supports with Mo and Co oxides and evaluated the resulting catalyst-adsorbents for simultaneous removal of 5,000 ppmv NH_3 and 10,000 ppmv H_2S at 650 °C. All catalyst-adsorbents had similar removal capacities for NH_3 alone but in the presence of H_2S only Co-Mo-Al_2O_3 showed effectiveness in decomposition of NH_3. These authors reported an H_2S adsorption capacity of 176 mg g^{-1} and an NH_3 removal percentage of 95% but no information on adsorption capacity of NH_3 was provided. Studying the simultaneous removal of toluene, NH_3 and H_2S from biomass-generated producer gas that contained 300 ppmv NH_3 and 150 ppmv H_2S, Bhandari et al. [3] employed a Mo and Al mixed metal oxide catalyst-adsorbent and achieved NH_3 and H_2S adsorption capacities of 8 and 30 mg g^{-1}, respectively at 800 °C. Comparing these results with those obtained with biochar and activated carbon, Bhandari et al. [3] concluded that NH_3 adsorption capacities of activated carbon and mixed metal oxide catalyst were much higher than that of biochar, whereas H_2S adsorption capacity of mixed metal oxide was higher than activated carbon and biochar.

The overview of the recent literature, provided here, clearly shows the lack of information on simultaneous removal of NH_3 and H_2S at low concentration and temperature range that are encountered in many practical situations such as emissions from livestock operations, wastewater treatment plants and landfills, and in raw biogas. Moreover, one can notice that in none of the earlier works impacts of NH_3 and H_2S concentrations and temperature on simultaneous adsorption NH_3 and H_2S have been investigated. The results of the present study indicate that the developed carbon-based adsorbent with relatively low metal oxides loading is a suitable candidate for the adsorptive removal of NH_3 and H_2S in applications where low gas concentrations and temperatures are encountered.

4 Conclusion

The findings of the present study on simultaneous adsorption of NH_3 and H_2S by activated carbon-based composite adsorbents, revealed that among the three synthesized adsorbents with ZnO and TiO_2 loadings of ~10 and 5%, 15 and 5%, and 15 and 10%, the composite with 10% ZnO and 5%TiO_2 (10ZnO-5TiO_2-AC) had the highest equilibrium adsorption capacities for NH_3 and H_2S, while the corresponding values for the other composites were close. Detailed evaluation of selected adsorbent (10ZnO-5TiO_2-AC) for simultaneous adsorption of NH_3 and H_2S under various gas concentrations and low temperature range revealed that equilibrium adsorption capacity for NH_3 increased with the increase of NH_3 concentration, but temperature had an opposing effect and lower adsorption capacities were obtained with the increase of temperature. In the case of H_2S, increase of concentration and temperature both enhanced the equilibrium adsorption capacity. These trends were consistent with those reported for a mixture of pure (commercial) TiO_2 and ZnO nanoparticles when applied for simultaneous removal of NH_3 and H_2S. The multicomponent Langmuir isotherm described the equilibrium data for adsorption of NH_3 and H_2S with high level of accuracy. The negative value of adsorption enthalpy for NH_3 confirmed the exothermic and potentially physical nature of ammonia adsorption, while in the case of H_2S a positive value of adsorption enthalpy revealed the endothermic and chemisorption nature of the adsorption process. The chemical nature of H_2S adsorption was also confirmed through examination of fresh and exposed adsorbents by XRD and FTIR that clearly showed representative peak for ZnS, a product of H_2S and ZnO reaction. Although mixture of pure (commercial) TiO_2 and ZnO nanoparticles provides higher adsorption capacities when compared to the composite adsorbent, the challenges associated with the use and handling of pure nanoparticles and their cost, makes the carbon-based composite adsorbent developed in this work a more feasible and practical choice for the large-scale capture of NH_3 and H_2S from gaseous emissions.

Acknowledgements This work was made possible by an Agriculture Development Fund grant (ADF 20140246) from the Ministry of

Agriculture, Government of Saskatchewan. Technical assistance of R. Blondin, and R. Prokopishyn from the Department of Chemical and Biological Engineering, University of Saskatchewan is gratefully acknowledged.

Author contributions Guadalupe Montserrat Valdes Labrada: Methodology, Investigation, Data interpretation and validation. Ruth Azar: Methodology, Investigation, Data interpretation and validation.Bernardo Predicala: Conceptualization, Methodology, Co-supervision. Mehdi Nemati: Conceptualization, Methodology, Co-supervision, Research management, Writing-first draft, revisions, submission, and correspondence. All authors contributed in writing the manuscript.

Funding Agriculture Development Fund grant (ADF 20140246), Ministry of Agriculture, Government of Saskatchewan, Canada.

Declarations

Ethical approval Not applicable.

Competing interests The authors declare no competing interests.

References

1 Agorku, E.S., Mamo, M.A., Mamba, B.B., Pandey, A.C., Mishra, A.K.: Cobalt-doped ZnS-reduced graphene oxide nanocomposite as an advanced photocatalytic material. J. Porous Mater. 2014. **22**(1 22), 47–56 (2014). https://doi.org/10.1007/S10934-014-9871-Y

2 Alinezhad, E., Haghighi, M., Rahmani, F., Keshizadeh, H., Abdi, M., Naddafi, K.: Technical and economic investigation of chemical scrubber and bio-filtration in removal of H_2S and NH_3 from wastewater treatment plant. J. Environ. Manage. **241**, 32–43 (2019). https://doi.org/10.1016/j.jenvman.2019.04.003

3 Bhandari, P.N., Kumar, A., Huhnke, R.L.: Simultaneous removal of toluene (model tar), NH_3, and H 2S, from biomass-generated producer gas using biochar-based and mixed-metal oxide catalysts. In: Energy and Fuels. pp 1918–1925 (2014)

4 Chellappa, M., Anjaneyulu, U., Manivasagam, G., Vijayalakshmi, U.: Preparation and evaluation of the cytotoxic nature of TiO_2 nanoparticles by direct contact method. Int. J. Nanomed. **10**, 31–41 (2015). https://doi.org/10.2147/IJN.S79978

5 Das, J., Nolan, S., Lens, P.N.L.: Simultaneous removal of H_2S and NH_3 from raw biogas in hollow fibre membrane bioreactors. Environ. Technol. Innov. **28** (2022). https://doi.org/10.1016/j.eti.2022.102777

6 Elizabeth, M., Cecil, K.K., Talam, E.K.: Hydrogen sulfide and ammonia removal from biogas using water hyacinth-derived carbon nanomaterials. Afr. J. Environ. Sci. Technol. **11**(7), 375–383 (2017). https://doi.org/10.5897/ajest2016.2246

7 Foo, K.Y., Hameed, B.H.: Decontamination of textile wastewater via TiO_2 /activated carbon composite materials. Adv. Colloid Interface Sci. **159**(2), 130–143 (2010). https://doi.org/10.1016/J.CIS.2010.06.002

8 Gandu, B., Palanivel, S., Juntupally, S., Arelli, V., Begum, S., Anupoju, G.R.: Removal of NH_3 and H_2S from odor causing tannery emissions using biological filters: Impact of operational strategy on the performance of a pilot-scale bio-filter. J. Environ. Sci. Health Part. A. **56**(6), 625–634 (2021). https://doi.org/10.1080/10934529.2021.1903283

9 Hernández, J., Dorado, A.D., Lafuente, J., Gamisans, X., Prado, Ó.J., Gabriel, D.: Characterization and evaluation of poplar and pine wood in twin biotrickling filters treating a mixture of NH_3, H_2S, butyric acid, and ethylmercaptan. Environ. Progress Sustainable Energy. **36**(1), 171–179 (2017). https://doi.org/10.1002/ep.12491

10 Huan, C., Fang, J., Tong, X., Zeng, Y., Liu, Y., Jiang, X., Ji, G., Xu, L., Lyu, Q., Yan, Z.: Simultaneous elimination of H_2S and NH_3 in a biotrickling filter packed with polyhedral spheres and best efficiency in compost deodorization. J. Clean. Prod. **284**, 124708 (2021). https://doi.org/10.1016/j.jclepro.2020.124708

11 Jamil, T.S., Ghaly, M.Y., Fathy, N.A., Abd El-Halim, T.A., Österlund, L.: Enhancement of TiO_2 behavior on photocatalytic oxidation of MO dye using TiO_2/AC under visible irradiation and sunlight radiation. Sep. Purif. Technol. **98**, 270–279 (2012). https://doi.org/10.1016/J.SEPPUR.2012.06.018

12 Jamshidi, M., Ghaedi, M., Dashtian, K., Ghaedi, A.M., Hajati, S., Goudarzi, A., Alipanahpour, E.: Highly efficient simultaneous ultrasonic assisted adsorption of brilliant green and eosin B onto ZnS nanoparticles loaded activated carbon: Artificial neural network modeling and central composite design optimization. Spectrochim. Acta Part A Mol. Biomol. Spectrosc. **153**, 257–267 (2016). https://doi.org/10.1016/J.SAA.2015.08.024

13 Jiang, Q., Li, T., He, Y., Wu, Y., Zhang, J., Jiang, M.: Simultaneous removal of hydrogen sulfide and ammonia in the gas phase: A review. Environ. Chem. Lett. **20**, 1403–1419 (2022)

14 Jung, S.Y., Lee, S.J., Park, J.J., Lee, S.C., Jun, H.K., Lee, T.J., Ryu, C.K., Kim, J.C.: The simultaneous removal of hydrogen sulfide and ammonia over zinc-based dry sorbent supported on alumina. Sep. Purif. Technol. **63**(2), 297–302 (2008). https://doi.org/10.1016/J.SEPPUR.2008.05.013

15 Lim, E.J., Jung, S.Y., Lee, S.C., Kim, J.C.: Enhancing the effect of CoAl2O4 on the simultaneous removal of H_2S and NH_3 on Co- and Mo- based catal-sorbents in IGCC. Sep. Purif. Technol. **177**, 94–100 (2017). https://doi.org/10.1016/j.seppur.2016.11.055

16 Lu, X., Jiang, J., Sun, K., Cui, D.: Characterization and photocatalytic activity of Zn2+–TiO_2/AC composite photocatalyst. Appl. Surf. Sci. **258**(5), 1656–1661 (2011). https://doi.org/10.1016/J.APSUSC.2011.09.042

17 Makarova, O., Rajh, T., Thurnauer, M.C., Martin, A., Kemme, P.A., Cropek, D.: Surface modification of TiO_2 nanoparticles for photochemical reduction of nitrobenzene. Environ. Sci. Technol. **34**(22), 4797–4803 (2000). https://doi.org/10.1021/es001109+

18 Neelgund, G.M., Oki, A.: Photothermal effect: An important aspect for the enhancement of photocatalytic activity under illumination by NIR radiation. Mater. Chem. Front. **2**(1), 64–75 (2017). https://doi.org/10.1039/C7QM00337D

19 Ouzzine, M., Romero-Anaya, A.J., Lillo-Ródenas, M.A., Linares-Solano, A.: Spherical activated carbon as an enhanced support for TiO_2/AC photocatalysts. Carbon. **67**, 104–118 (2014). https://doi.org/10.1016/J.CARBON.2013.09.069

20 Park, J.J., Park, C.G., Jung, S.Y., Lee, S.C., Ragupathy, D., Kim, J.C.: A study on Zn-based catal-sorbents for the simultaneous removal of hydrogen sulfide and ammonia at high temperature. In: Research on Chemical Intermediates. pp 1193–1202 (2011)

21 Piña-Pérez, Y., Aguilar-Martínez, O., Acevedo-Peña, P., Santolalla-Vargas, C.E., Oros-Ruíz, S., Galindo-Hernández, F., Gómez, R., Tzompantzi, F.: Novel ZnS-ZnO composite synthesized by the solvothermal method through the partial sulfidation of ZnO for H2 production without sacrificial agent. Appl. Catal. B. **230**, 125–134 (2018). https://doi.org/10.1016/J.APCATB.2018.02.047

22 Rezaei, E., Azar, R., Nemati, M., Predicala, B.: Gas phase adsorption of ammonia using nano TiO_2-activated carbon composites – effect of TiO_2 loading and composite characterization. J. Environ. Chem. Eng. **5**(6), 5902–5911 (2017a). https://doi.org/10.1016/J.JECE.2017.11.010

23 Rezaei, E., Schlageter, B., Nemati, M., Predicala, B.: Evaluation of metal oxide nanoparticles for adsorption of gas phase

ammonia. J. Environ. Chem. Eng. **5**(1), 422–431 (2017b). https://doi.org/10.1016/J.JECE.2016.12.026

24 Rosso, I., Galletti, C., Bizzi, M., Saracco, G., Specchia, V.: Zinc oxide sorbents for the removal of hydrogen sulfide from syngas. Ind. Eng. Chem. Res. **42**(8), 1688–1697 (2003). https://doi.org/10.1021/ie0208467

25 Song, H.S., Park, M.G., Kwon, S.J., Yi, K.B., Croiset, E., Chen, Z., Nam, S.C.: Hydrogen sulfide adsorption on nano-sized zinc oxide/reduced graphite oxide composite at ambient condition. Appl. Surf. Sci. **276**, 646–652 (2013). https://doi.org/10.1016/J.APSUSC.2013.03.147

26 Valdes Labrada, G.M., Kumar, S., Azar, R., Predicala, B., Nemati, M.: Simultaneous capture of NH_3 and H_2S using TiO < inf > 2 and ZnO nanoparticles - laboratory evaluation and application in a livestock facility. J. Environ. Chem. Eng. **8**(1) (2020). https://doi.org/10.1016/j.jece.2019.103615

27 Xue, G., Liu, H., Chen, Q., Hills, C., Tyrer, M., Innocent, F.: Synergy between surface adsorption and photocatalysis during degradation of humic acid on TiO_2/activated carbon composites. J. Hazard. Mater. **186**(1), 765–772 (2011). https://doi.org/10.1016/J.JHAZMAT.2010.11.063

28 Zhang, Z., Xu, Y., Ma, X., Li, F., Liu, D., Chen, Z., Zhang, F., Dionysiou, D.D.: Microwave degradation of methyl orange dye in aqueous solution in the presence of nano-TiO_2-supported activated carbon (supported-TiO_2/AC/MW). J. Hazard. Mater. **209–210**, 271–277 (2012). https://doi.org/10.1016/J.JHAZMAT.2012.01.021

29 Zheng, T., Li, L., Chai, F., Wang, Y.: Factors impacting the performance and microbial populations of three biofilters for co-treatment of H_2S and NH_3 in a domestic waste landfill site. Process Saf. Environ. Prot. **149**, 410–421 (2021). https://doi.org/10.1016/j.psep.2020.11.009